

Photodegradation of 4BS Dye Over Pd-doped TiO₂ Synthesized By EDTA-Glycol Method

M.J. Pawar*, V.B. Nimbalkar, A.D. Khajone, M.D. Gaonar

Laboratory of Materials Synthesis, Smt. Narsamma ACS College, Kiran Nagar, Amravati M.S. India

Abstract

We report in this chapter photocatalytic activity of Pd-doped TiO₂ nanoparticles under visible light irradiation synthesized by using an EDTA-Glycol method. Structural, morphological, and basic optical properties of these samples were investigated using X-ray diffraction (XRD), scanning electron microscopy (SEM) and UV-Vis reflectance. Room temperature X-ray diffraction analysis revealed that Pd-doped TiO₂ has both anatase and brookite phases, but TiO₂ sample doped 2wt% Pd only have the anatase phase. The morphologies of TiO₂ were influenced by doping with Pd, as shown from the SEM images. UV-Vis reflectance results show decreased band gap energy of Pd-doped TiO₂ in comparison to that of pure TiO₂. The present research work is mainly focused on the enhancement of degradation efficiency of Fast Scarlet 4BS by doping of Pd in TiO₂ matrix using UV-light (365nm). A 99.5% photodegradation of methylene blue was achieved by utilizing 0.25mol% Pd-doped TiO₂ (1 g/L) at pH = 3 within 70min.

Keywords: TiO₂; Pd-doped TiO₂; Photodegradation; 4BS Dye

Date of Submission: 10-10-2021

Date of Acceptance: 24-10-2021

I. Introduction

The semiconductors TiO₂, ZnO, SrTiO₃, CeO₂, WO₃, Fe₂O₃, GaN, Bi₂S₃, CdS and ZnS can all act as photoactive materials for redox/charge-transfer processes due to their electronic structures which are characterized by a filled valence band and an empty conduction band. Among the simple oxides (e.g. TiO₂, ZnO, WO₃, Fe₂O₃), anatase phase of TiO₂ is the dominant structure employed for sunlight applications mostly due to its charge carrier handling properties and exhibit the adequate conversion values [1-12]. However, in spite of its high conversion values, the calculated quantum yield for these reactions studied is appreciably low: certainly well below 10% for most degradation and synthesis processes [12]. The catalytic activity of TiO₂ is independent of its crystal structure, crystal size distribution, surface roughness, surface hydroxyl group density, and so on [13].

However, the TiO₂ photocatalyst is known to have limitations for practical applications. One of these limitations is that the TiO₂ has activity only under light of wavelength shorter than 388 nm because of its wide band gap (E_g = 3.2 eV) [14-16]. The wide band gap limits the use of sunlight as excitation energy and the high rate of recombination of photo-generated electron-hole pairs in TiO₂ results in low photocatalytic efficiency. To overcome these two difficulties, many efforts have been made to modify TiO₂ nanoparticles [17-19]. One of the promising approaches is based on the metal loading. Various metals, such as Pt, Au, Pd, Rh and Ag, have been used as electron acceptors to separate the photo-induced hole/electron pair and promote interfacial charge-transfer processes [20-24]. Therefore, the aim of the present work is to study the effect of palladium on the properties and activity of the TiO₂ photocatalyst prepared by the EDTA-Glycol method. To investigate the photocatalytic efficiency of the pure and doped TiO₂, water-soluble C.I. Direct Red 23 known also as Fast Scarlet 4BS (abbreviated as 4BS in the present study) dye was used as a model pollutant.

II. Experimental

2.1 Synthesis of pure and Pd-doped TiO₂

The precursor solution was prepared by dissolving titanium tetraisopropoxide (TTIP) in the glacial acetic acid (AA), followed by the addition of double distilled water. Then the solution of salt of ethylene diamine tetraacetic acid (EDTA) was added to this mixture and the mixture was stirred for 60 min at 60°C. After 60 min, to the stirred mixture, ethylene glycol (EG) was added and stirring was continued for further 60 min at 60°C. The mol ratio of TTIP:EG must be kept at 1:1 and 1:2. The obtained material was calcined at 500°C to get pure TiO₂ coded as TiO. Then, 1M Pd solution was added drop wise into the precursor solution for a few minutes in order to get the samples Pd1TiO and Pd2TiO with Pd wt% of 0.1 and 0.2 respectively. The solution was dried at the temperature of 80°C overnight. The dried gel was grinded and calcined in a muffle furnace at 500°C for 4 h. To study the effect of fuel quantity on the TiO₂, the volume of EG was doubled

and the similar method was adopted for the sample preparation.

2.3 Photocatalytic Decolorization of 4BS

The photocatalytic reactivity of pure and Pd-doped TiO₂ was evaluated by the decolorization of 4BS under visible light irradiation. A LED lamp of 15 W was used as a light source for testing. Different amounts of the pure and Pd-doped TiO₂ powder were added into 25 ml of 20 mg/L MB solution. Before open LED light, the suspension was put in the reactor and stirred until dye adsorption was completed. After that, the LED light was turned on. The concentration of 4BS dye solution was evaluated at given time intervals of every 30 min by using UV-vis spectrophotometry at wavelength of 650 nm (λ_{max}).

III. Result and discussion

3.1 XRD analysis

The X-ray diffraction patterns of the undoped and 0.0%, 0.1%, and 0.2% palladium doped TiO₂ calcined at 450°C is presented in Figure 1. This figure indicates that the sample calcined at 450°C consists of both anatase and brookite phases. The XRD patterns didn't show any Pd phase even for the 0.2% Pd doped TiO₂. This may reveal that Pd ions are uniformly dispersed in TiO₂ matrix. The shape of diffraction peaks of the crystal planes of pure TiO₂ is quite similar to those of Pd-doped TiO₂ of different Pd concentrations. Substantially, the enlarged peaks at (101) plane (JCPDS number-21-1272) and (121) plane for the samples Figures 1b and 1c showed a slight shift to smaller angles with Pd incorporation. It indicates that Pd ions could enter into TiO₂ lattice or interstitial site. We know that the difference in ionic radius between palladium ion (Pd²⁺ = 0.11 nm) and titanium ion (Ti⁴⁺ = 0.064 nm) is large. The average crystal sizes of TiO₂ and Pd doped TiO₂ nanoparticles were calculated and also, were presented in Table 1. It was observed that, the average crystal size of the synthesized samples was significantly changed due to the addition of the Pd.

Table 1 Average crystallite size, specific surface area and pore size of pure and Pd-doped TiO₂ calcined at 450°C (TTIP:EG 1:1).

Sample	Pd wt%	Average crystallite size (nm) ^a	BET surface area (m ² g ⁻¹)	Pore size (nm) ^b
TiO	0.0	24.30	64.44	3.24
Pd1TiO	0.1	22.23	65.43	3.85
Pd2TiO	0.2	20.25	72.54	4.33

a = calculated from Scherrer equation; b = Calculated from S_{BET}

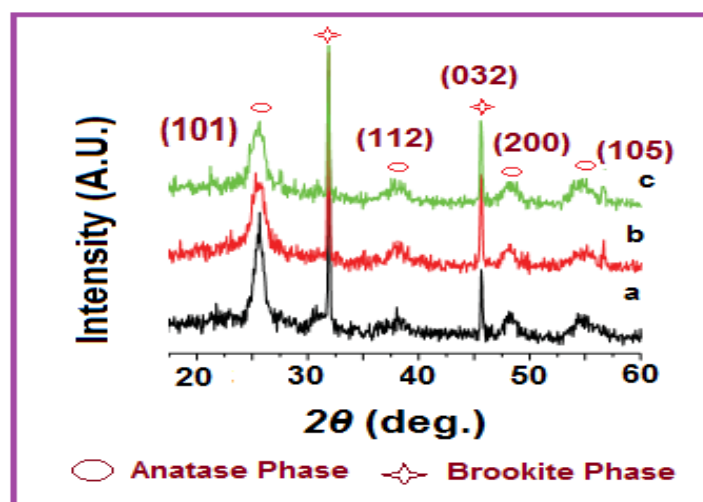


Figure 1. XRD patterns of pure and Pd-doped TiO₂ calcined at 500°C.

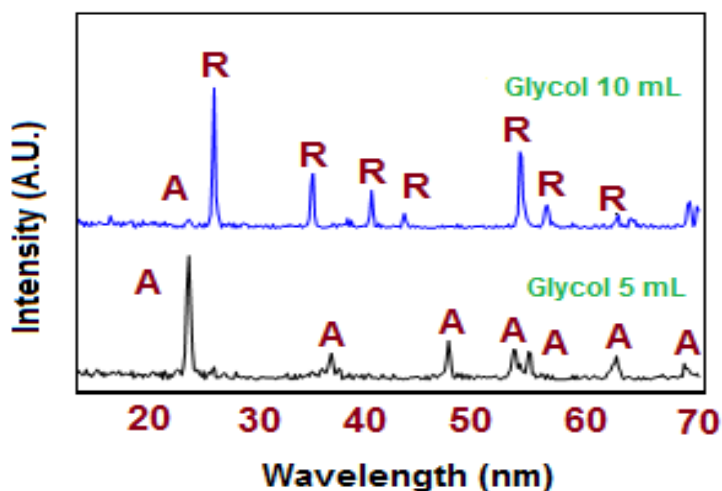


Figure 2 XRD patterns of pure and Pd-doped TiO₂ calcined at 500°C.

Further, we have synthesized Pd₂TiO sample by EDTA-Glycol method using the double volume of EG to investigate the influence of the amount of the fuel during combustion on the structure and the synthesized TiO₂ materials. The role of fuel quantity was also found to be crucial in determining the photocatalytic efficiency of TiO₂. XRD results are presented in Figure 2. From XRD results, it was observed that, on doubling the volume of glycol the drastic change in phase of TiO₂ was observed from anatase to rutile phase.

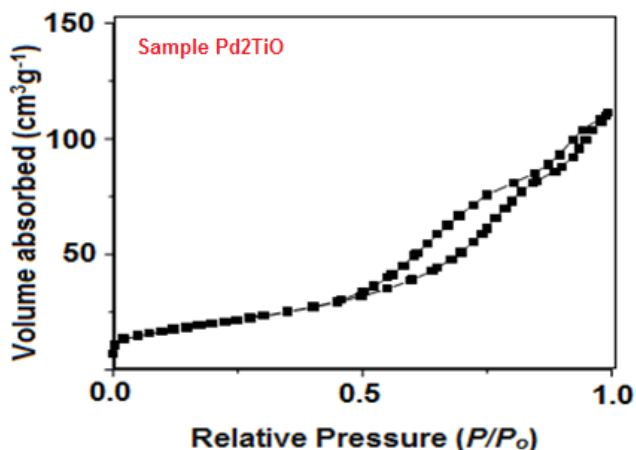


Figure 2. N₂ adsorption/desorption isotherm of Pd₂TiO sample calcined at 500°C.

3.2 N₂ adsorption studies

The surface textural characteristics of pure and Pd-doped samples are derived from N₂ adsorption analysis. Specific surface area (S_{BET}) by BET method, total pore volume calculated at $P/P_0=0.99$, and average pore diameter values are presented in Table 1. Figure 3 presents the adsorption isotherms of pure and Pd-doped samples. The samples showed type IV behaviour with the typical hysteresis loop. This hysteresis is a characteristic of mesoporous materials [25,26]. It can be seen in Table 1, that the doped sample had larger surface area and smaller average crystallite size than the undoped one. This might be due to the slight decrease of crystallite size for the Pd-doped TiO₂ as mentioned in XRD pattern.

3.3 UV-vis spectroscopy

Optical properties were observed by UV-vis spectroscopy. Figure 4 demonstrates the optical absorption spectra of pure and Pd-doped TiO₂ samples. The absorption edge of TiO₂ nanoparticles at 387 nm moved to a longer wavelength after doping with Pd-doping, showing the absorption edge at 432 nm for Pd₁TiO sample and 450 nm for Pd₂TiO sample. After doping with Pd the response of TiO₂ nanoparticles to visible light was increased and showed red shift. The red shift of the absorption curve results in a reduction of the band gap energy and also the recombination rate, and hence, enhanced photocatalytic activity.

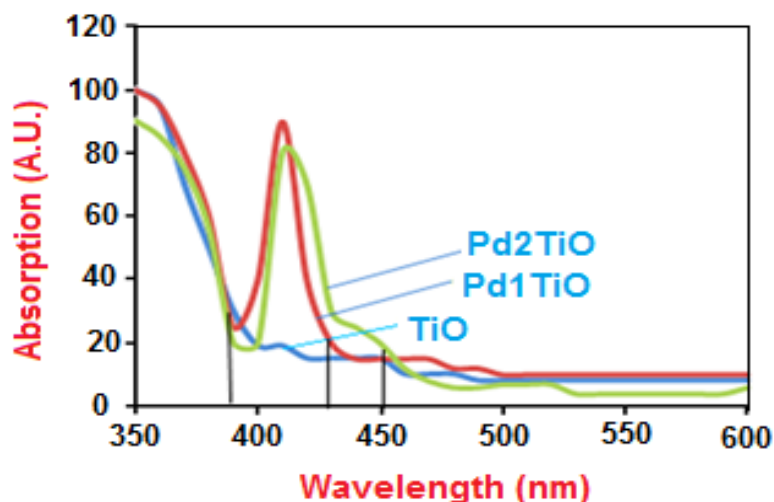


Figure 3. UV visible absorption spectra of pure and Pd-doped TiO₂ samples.

3.4 SEM and TEM studies

The micrographs of the TiO, Pd1TiO and Pd2TiO samples are shown in Figure 5. One can see the change in morphology and the surface structure of the pure and Pd-doped TiO₂ samples with increasing wt% of Pd. Figure 5 also shows the TEM result of the pure and Pd-doped TiO₂ nanoparticles calcined at 500°C. The TEM images also confirm the decrease in crystallite size with Pd doping in TiO₂ structure. The result of the TEM agrees with the XRD results concerning the particle size range.

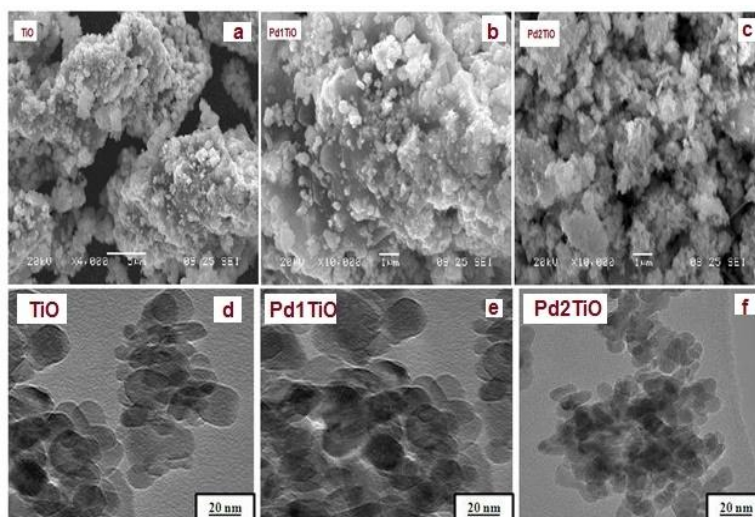


Figure 4 SEM and TEM images of pure and Pd-doped TiO₂.

3.5 Effect of Operating Parameters on the Photodegradation of 4BS

3.5.1 Effect of catalytic dose

Experiments were performed to study the variations in the rate of decolorization at different concentrations of catalyst, ranging from 1.0 to 3.0 g/L, at pH 12.0. It was observed that the photocatalytic decolorization efficiency of 4BS increased with an increasing amount of the photocatalyst, and reached the highest value when the concentration of pure and Pd-doped TiO₂ sample was 2 g/L and finally decreased, as shown in Figure 5. This phenomenon is similar to that found in the study of other photocatalysts, such as TiO₂ and ZnO [27]. The enhancement of the removal rate may be due to the increase in the availability of active sites, which increases the number of dye molecules adsorbed, and the increase in the density of particles in the area of illumination. At higher catalyst loading, the percentage of degradation decreases because of the deactivation of activated molecules by agglomeration, which decreases the radiation penetration and increases the radiation scattering in dye the solution. The best amount of catalyst must be added in order to avoid unnecessary excess catalyst and to ensure the maximum photodegradation of dye.

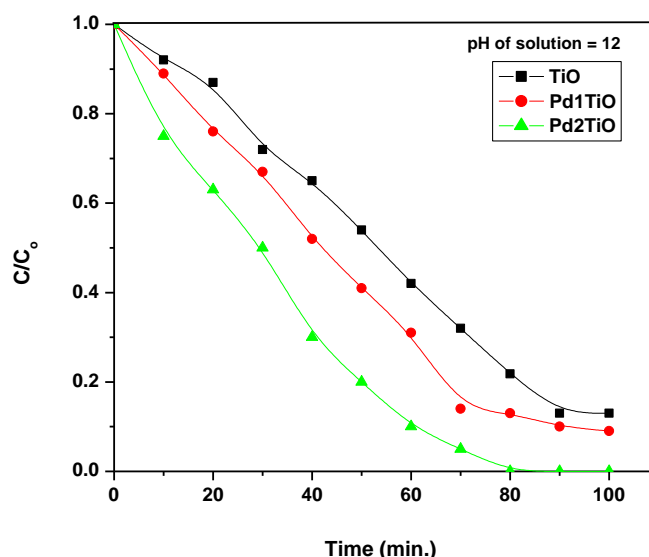


Figure 5 Effect of catalyst dose on photocatalytic degradation of 4BS over pure and Pd-doped TiO₂.

3.5.2 Effect of pH

The effect of pH from 4.0 to 12.0 on the decolorization at constant air flux, a temperature of 25°C with 2 g of Pd2TiO the catalyst for 90 min is illustrated in Figure 6. The worst results were obtained at pH 7.0 and acidic and alkaline pH values were favored. The photocatalytic removal of color was observed to be faster at alkaline pH than at acidic pH. The best pH was 12.0.

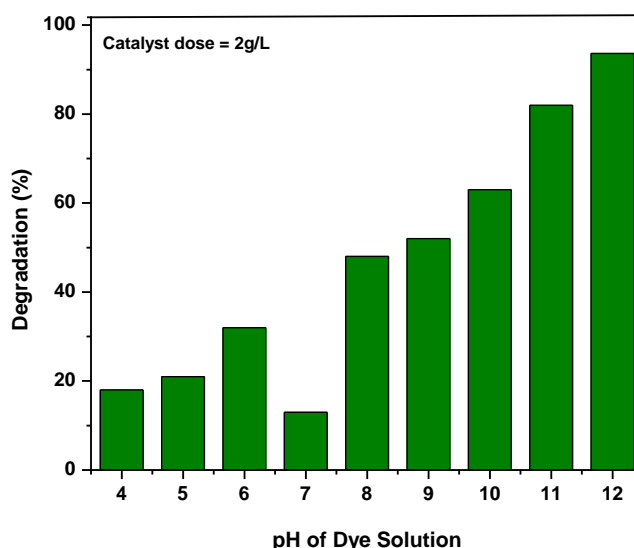


Figure 6 Effect of pH of dye solution on 4BS degradation over Pd2TiO.

3.5.3 Effect of initial concentration of dye

The effect of the initial concentration of dye on the rate of decolorization was studied by varying the initial dye concentration from 100 to 500 mg/L at pH 12.0, with a constant intensity of 250W and a catalyst loading of 2 g/L, as shown in Figure 7. It was observed that, the photodegradation of 4BS dye decreases with increasing initial concentration of dye. These results presented in Figure 7 are in good agreement with the results of the studies reported by Neppolian et al. [28] and Toor et al. [29]. The rate of dye degradation relates to the probability of formation of OH radicals on the surface of the catalyst and to the probability of OH radicals reacting with dye molecules. As the initial concentration increases, the active sites of the catalyst are covered by dye ions and the path-length of photons entering the solution decreases. In low concentrations, however, the

reverse effect is observed; consequently, the number of OH radicals formed on the surface of catalyst increases, the relative number of OH radicals attacking the compound increases, and thus the photodegradation efficiency increases. Another possible cause for such results is the UV-screening effect of the dye itself. At a high concentration of dye, a significant amount of UV light may be absorbed by the dye molecules rather than the catalyst particles, and that reduces the efficiency of the catalytic reaction because the concentrations of •OH and O₂^{•-} decrease [31].

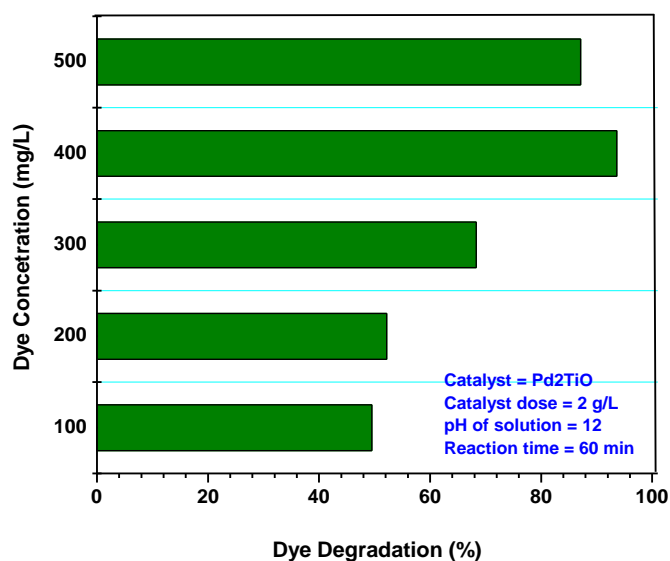


Figure 7 Effect of initial concentration of dye on 4BS degradation over Pd₂TiO.

3.5.4 Effect of scavenger

Iodide ion acts as a scavenger that reacts with positive holes and surface hydroxyl radicals, reducing the dye degrading efficiency of photocatalyst. In the present investigation, the 4BS dye solution (dose = 400 mg/L, pH of solution = pH 12.0) mixed with scavenger KI (0–40 mmol/L) was irradiated for 60 min with 2 g/L of Pd₂TiO. Figure 8 shows the change of photocatalytic decolorization of 4BS with increasing KI concentration. Obviously, with the increase of the KI concentration, the rate of dye degradation decreases. Since iodide ion scavenged the positive holes and surface hydroxyl radicals on catalyst surface reduced the number of reactive species available for photodegradation of the adsorbed 4BS. In addition, iodide ion completed the adsorptive sites on the Pd₂TiO surface, resulting in the decreased dye degradation efficiency.

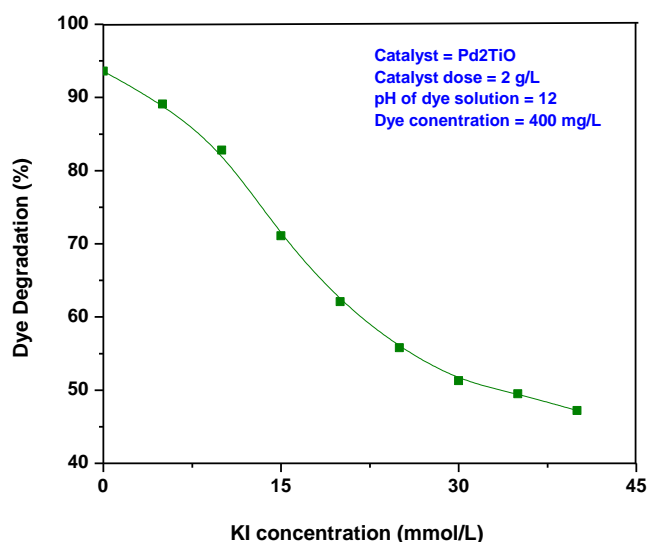


Figure 8 Effect of KI concentrations as a scavenger on 4BS dye degradation over Pd₂TiO catalyst.

IV. Conclusion

The pure and Pd-doped TiO₂ nanoparticles were prepared by the EDTA-Glycol method using ethylene glycol as a fuel. Samples prepared by calcinations at 500°C contain anatase phase only. If the volume of ethylene glycol is doubled, the percentage of rutile phase increases dramatically. Doping TiO₂ with palladium has no significant effect on the particle sizes and did not result in the formation of a new crystalline phase. It was confirmed that the incorporation of Pd in TiO₂ matrix shifts the onset wave length of absorption to higher values. The pure TiO₂ exhibited lower efficiency than the Pd-doped TiO₂ for 4BS dye solution and the photocatalytic efficiency increases with increasing palladium content up to 0.2wt%. At pH = 12, about 95% degradation of 4BS was with 2 g/L of Pd₂TiO dose. Further studies to improve the metal loading can lead to the production of even more efficient materials for photocatalytic applications.

References

- [1]. Hoffmann, M. R., Martin, B. T., Choi, W., Bahnemann D. W., Environmental Applications of Semiconductor Photocatalysis, Chem. Rev. 95, 69, (1995).
- [2]. Anpo, M.; Tacheuchi, M. J. Catal. The design and development of highly reactive titanium oxide photocatalysts operating under visible light irradiation, 216, 505 (2003).
- [3]. Hermann, J. M., Heterogeneous photocatalysis: state of the art and present applications In honor of Pr. R.L. Burwell, Topics Catal. 34, 49, (2005).
- [4]. Bahnemann, D. W.; Anpo, M. Sol. Energy 77, 445 (2004).
- [5]. Thompson, T. L., Yates, J. T., Surface Science Studies of the Photoactivation of TiO₂ New Photochemical Processes, Chem. Rev. 106, 4428, (2006).
- [6]. Serpone, N. J., Is the Band Gap of Pristine TiO₂ Narrowed by Anion- and Cation-Doping of Titanium Dioxide in Second-Generation Photocatalysts? Phys. Chem. B 110, 24287, (2006).
- [7]. Colon, G., Belver, C., Fernandez-García, M., Nanostructured oxides in Photocatalysis. In Synthesis, Properties and Applications of Solid Oxides; Rodríguez, J. A., Fernandez-García, M., Eds.; Wiley: New York (2007).
- [8]. Carp, O., Huisman, C. L., Reller, A., Prog. A., Photoinduced reactivity of titanium dioxide Solid State Chem. 32, 33, (2004)
- [9]. Di Valentin, C., Diebold, U., Selloni, A., Chem. Phys. Lett., 339, and articles therein. (2007).
- [10]. Zhang, H., Chen, G., Bahnemann, D. W., Mater. J. Chem. Photoelectrocatalytic materials for environmental applications 19, 5085, (2009).
- [11]. Fox, M. A.; Dulay, M. T. Heterogeneous photocatalysis, Chem. Rev. 1993, 93, 341, (1993).
- [12]. Hincapie, M., Maldonado, M., Oller I, Gernjak I. W., Sanchez-Perez S., Ballesteros J.A., Malato M.M., Catal. S. Today 101, 203, (2005).
- [13]. Sonawane R. S, Kale B. B., and Dongare M. K., 2004 Mater. Chem. Phys. 85 52, (2004).
- [14]. GeL, Xu M.X., "Influences of the Pd Doping on the Visible Light Photocatalytic Activities of InVO₄-TiO₂ Thin Films," Materials Science and Engineering: B, Vol. 131, No. 1-3, 222-229 (2006).
- [15]. Xie B.P., Xiong Y., Chen R.M., Chen J., Cai P.X., "Catalytic Activities of Pd-TiO₂ Film towards the Oxidation of Formic Acid," Catalysis Communications, Vol. 6, No. 11, 699-704, (2005).
- [16]. Zhang X., Zhang F., Chan K.Y., "The Synthesis of Pt-Modified Titanium Dioxide Thin Films by Micro emulsion Templating, Their Characterization and Visible- Light Photocatalytic Properties," Materials Chemistry and Physics, Vol. 97, No. 2-3, 384-389, (2006).
- [17]. Li H., Zhu B.L., Feng Y.F., Wang S. R., Zhang S.M. and Huang Z.P., "Synthesis, Characterization of TiO₂ Nanotubes-Supported MS (TiO₂NTs@MS, M = Cd, Zn) and Their Photocatalytic Activity," Journal of Solid State Chemistry, Vol. 180, No. 7, 2136-2142, (2007).
- [18]. Geng W.T. and Kim K.S., "Interplay of Local Structure and Magnetism in Co-Doped TiO₂ Anatase," Solid State Communications, Vol. 129, No. 11, 741-746 (2004).
- [19]. Wu J. C.-S. and Chen C.-H., "A Visible-Light Response Vanadium-Doped Titania Nano catalyst by Sol-Gel Method," Journal of Photochemistry and Photobiology A: Chemistry, Vol. 163, No. 3, 509-515 (2004).
- [20]. Strukul G., Gavagnin R., Pinna F., Modaferrri E., Perathoner S., Centi G., Marella M. and Tomaselli M., "Use of Palladium Based Catalysts in the Hydrogenation of Nitrates in Drinking Water: From Powders to Membranes," Catalysis Today, Vol. 55, No. 1-2, 139-149, (2000).
- [21]. Castillo S., Lopez T., "Catalytic Reduction of Nitric Oxide on Pt and Rh Catalysts Supported on Alumina and Titania Synthesized by the Sol-Gel Method," Applied Catalysis B: Environmental, Vol. 15, No. 3-4, 203-209 (1998).
- [22]. Lopeze T., Gomez R., Pecci G., Reyes P., Bokhimi X. and Novaro O., "Effect of pH on the Incorporation of Platinum into the Lattice of Sol-Gel Titania Phases," Materials Letters, Vol. 40, No. 2, 59-65 (1999).
- [23]. Matsuoka J., Naruse R., Nasu H. and Kamiya K., "Preparation of Gold Microcrystal-Doped Oxide Optical Coatings through Adsorption of Tetrachloroaurate Ions on Gel Films," Journal of Non-Crystalline Solid., Vol. 218, 151-155, (1997).
- [24]. Kingery W. D., Bowen H. K. and Uhlmann D. R., "Introduction to Ceramics," 2nd Edition, John Wiley and Sons, New York, 457, (1976).
- [25]. Gregg S. J. and Sing K. S. W., Adsorption, Surface Area and Porosity Academic Press, London, UK, 2nd edition, (1982).
- [26]. Xu J., Chen M., Fu D., "Study on highly visible light active Bi-doped TiO₂ composite hollow sphere," Applied Surface Science, vol. 257, no. 17, 7381-7386, (2011).
- [27]. Habibi M.H., Hassanzadeh A., Mahdavi S., The effect of operational parameters on the photocatalytic degradation of three textile azo dyes in aqueous TiO₂ suspension, J. Photochem. Photobiol. A 172, 89-96, (2005).
- [28]. Mills A., Davies R.H., Worsley D., Water-purification by semiconductor photocatalysis, Chem. Soc. Rev. 22 417-425, (1993).
- [29]. Fox M.A., Dulay M.T., Heterogeneous photocatalysis, Chem. Rev. 93, 341-357, (1993).
- [30]. Konstantinou I.K., Albanis T.A., TiO₂-assisted photocatalytic degradation of azo dyes in aqueous solution: kinetic and mechanistic investigations: a review, Appl. Catal. B 49 1-14, (2004).
- [31]. Toor A.P., Verma A., Jotshi C.K., Bajpai P.K., Singh V., Photocatalytic degradation of Direct Yellow 12 dye using UV/TiO₂ in a shallow pond slurry reactor, Dyes Pigments 68, 53-60 (2006).